



Microwave assisted polyol method for the preparation of Pt/C, Ru/C and PtRu/C nanoparticles and its application in electrooxidation of methanol

Srinivasan Harish^{a,b}, Stève Baranton^a, Christophe Coutanceau^{a,*}, James Joseph^b

^a Université de Poitiers, IC2MP, UMR CNRS 7285, 4 rue Michel Brunet B27, 86022 Poitiers cedex, France

^b Electrodes and Electrocatalysis Division, CSIR – Central Electrochemical Research Institute, Karaikudi, Tamilnadu, India

ARTICLE INFO

Article history:

Received 16 January 2012

Received in revised form

16 March 2012

Accepted 1 April 2012

Available online 25 April 2012

Keywords:

CO stripping

Methanol oxidation

Microwave activation

Platinum

Polyol method

Ruthenium

ABSTRACT

A polyol process activated by microwave irradiation was implemented to prepare efficient Pt/C, Ru/C and Pt₁Ru₁/C electrocatalysts for methanol oxidation with reducing synthesis cost and time. Study of the post-synthesis mixture by UV–visible spectroscopy led to determine the minimum batch temperature and synthesis time necessary for the complete reduction of metal salts. It was shown that disappearance of metal salts and colloid formation took place after 5 min at 100 °C for Pt, 5 min at 130 °C for Ru and 5 min at 160 °C for Pt₁Ru₁. The PtRu catalyst characterizations by TGA, TEM and XRD indicated that the nominal loading and nominal composition were achieved, and that the structure of this material consisted of a mixture of Pt_{0.8}Ru_{0.2} monocrystalline particles of ca. 2.5–3.0 nm, RuO₂ nanoclusters and probably Ru nanoclusters. Pt₁Ru₁/C catalyst displayed a high activity towards CO and methanol electrooxidation, with onset potentials of ca. 0.2 V lower than those obtained on Pt/C catalysts, and a low surface poisoning at 0.6 V vs. as demonstrated by chronoamperometry measurement RHE and in situ infrared reflectance spectroscopy.

© 2012 Elsevier B.V. All rights reserved.

1. Introduction

The application of fuel cell is currently limited by inadequacy in materials performance. Sir William Grove had already stated in 1839 [1] that “the chief difficulty was to obtain anything like a notably surface for action”. For this reason, nanosized particles of platinum and platinum–ruthenium supported on carbon are still the most used electrocatalysts in Proton Exchange Membrane Fuel Cell (PEMFC) and Direct Methanol Fuel Cell (DMFC) electrodes, respectively.

For obtaining such nanostructured catalysts, numerous synthesis methods were developed, including electrochemical deposition [2,3], physical vapour deposition [4], colloidal routes [5], impregnation reduction route [6], etc. Amongst the chemical methods, colloidal routes based on the use of organic surfactant as stabilizing agent are not industrially scalable methods. However, the polyol method has shown very promising potency for the preparation of Pt [7] and bimetallic Pt-based nanoparticles [8]. This method, well described by Fievet et al. [9], allows obtaining metal nanoparticles by reduction of metallic salts in ethylene glycol and can be performed without addition of any surfactant. So, the polyol

method uses inexpensive solvent (ethylene glycol), does not need the presence of surfactant to achieve well-dispersed catalytic particles of small mean sizes and is very easy to implement.

Bock et al. [10] have studied the synthesis of PtRu nanocatalysts via the polyol method. The reaction was performed at reflux at 160 °C for several hours. They showed that the reaction mechanism involved the oxidation of ethylene glycol to aldehyde and then to glycolic acid or, depending on the pH, to glycolate, while the Pt⁴⁺ and Ru³⁺ precursor salts were reduced. In the case of Pt/C catalyst synthesis, Liu et al. [11] explained that in the synthesis process the polyol solution containing the metal salt was refluxed at 120 °C–170 °C in order to decompose ethylene glycol and to generate *in situ* reducing species for the reduction of the metal ions to their elemental states. In traditional synthesis method, the reduction reaction is then activated by temperature: the synthesis is carried out by heating the reaction mixture at temperature higher than 120 °C for several hours [7,9,12,13].

Recently, Lebègue et al. [14] developed a method based on the activation reaction by microwave impulsion, which allowed energy and preparation time savings, to synthesize well-dispersed Pt/C catalyst of ca. 2.5 nm mean size, low size distribution, leading to high electrochemical surface area. These authors showed that such method leads to highly active Pt/C catalyst towards the oxygen reduction reaction and highlighted the effect of microwave activation at low temperature (80 °C and 100 °C) on the structure of Pt/

* Corresponding author. Tel.: +33 5 49 45 48 95; fax: +33 5 49 45 35 80.

E-mail address: christophe.coutanceau@univ-poitiers.fr (C. Coutanceau).

C catalysts, particularly on active surface area and metal loading on carbon.

The microwave dielectric heating leads to thermal and non-thermal effects [15]. Thermal effects arise from different temperature regimes under microwave heating, whereas non-thermal effects result from effects inherent to the microwaves [16]. These last authors showed that these effects lead to different morphologies and sizes of metallic nanostructures in comparison with those obtained by a conventional oil-bath heating. They also underlined that detailed mechanism for the preparation of metallic nanostructures under microwave irradiation has not been yet clarified. But, according to the generally admitted metal salt reduction mechanism via the formation of aldehyde intermediate during the polyol synthesis process, and considering that ethylene glycol possesses high dielectric losses and high reduction ability [16], it can be proposed that the role of microwave could be to favour the dehydrogenation of the molecule and hence the reduction of metallic salts. Anyway, the main advantages of microwave irradiation were discussed by Tsuji et al. [16]: the uniform heating of the solution leading to a more homogeneous nucleation and shorter crystallization time, a very short thermal induction period, the generation of localized high temperatures at the reaction sites resulting in enhancement of reduction rates of metallic ions and superheating of solvents over the boiling points as a consequence of the microwave dissipation over the whole liquid volume. Microwave dielectric loss heating appears then as a better synthesis option in view of its energy efficiency, preparation time saving, uniformity of heating across the whole solvent volume (no thermal convection), and implementation simplicity.

For these reasons, a polyol method activated by microwave irradiation was implemented in the present contribution in order to synthesize Pt/C and Pt₁Ru₁/C catalysts. The nanosized materials were characterized by TEM and XRD and their electro-catalytic behaviour towards electrooxidation of carbon monoxide and methanol was evaluated using cyclic voltammetry and *in situ* infrared study.

2. Experimental

2.1. Synthesis of the Pt/C, Ru/C and Pt₁Ru₁/C catalysts

Appropriate amounts of H₂PtCl₆·6H₂O and/or RuCl₃ (99.9% purity, Alfa Aesar) were dissolved in 100 mL of ethylene glycol (puriss. p.a., ≥99.5% Fluka) in order to reach a concentration of metals of 0.375 g L⁻¹ (Table 1). Then, pH of the solution was adjusted at 11 for the pure Pt sample and 10 for Ru containing catalysts by adding a solution of NaOH (1 M) in ethylene glycol drop wise. Carbon Vulcan XC72R (150 mg) thermally treated for 4 h at 400 °C under Nitrogen (U Quality from “Air Liquide”) was then added to the solution in order to obtain a nominal metal loading of 20 wt% on carbon and the mixture was ultrasonically homogenized for 5 min. The reactor equipped with a cooler was put inside a MARS oven from CEM Corporation. Such set up activates the synthesis reaction by microwave irradiation at atmospheric pressure, without evaporation of ethylene glycol and/or water due to

Table 1

Metal salt weights dissolved in 100 mL of ethylene glycol and corresponding concentration for the synthesis of catalysts loaded with 20 wt.% of metal. The carbon powder mass added is 150 mg.

	Metal salt weight/mg		Metal concentration/g L ⁻¹		Me/(Me + C) ratio/wt.%
	H ₂ PtCl ₆ ·6H ₂ O	RuCl ₃	Pt	Ru	
Pt/C	100		0.375		20
Ru/C		77		0.375	20
Pt ₁ Ru ₁ /C	66	26	0.248	0.128	20

temperature increase during microwave irradiation. The synthesis of catalysts was performed under continuous microwave irradiation at a power of 1600 W until reaching the desired reaction temperature, and then microwave pulses were applied to maintain it. Fig. 1 shows the schema representing the microwave sequence and corresponding solvent temperature profile during the synthesis process by pulsed microwaves.

The catalytic powders were washed with acetone and ultra pure water (MilliQ, Millipore, 18.2 MΩ cm), and filtrated. Finally, thermal treatment of Pt/C catalysts is performed at 160 °C [10] for 1 h under air to remove traces of ethylene glycol.

2.2. Physicochemical characterization of the Pt/C, Ru/C and Pt₁Ru₁/C catalysts

Thermogravimetric analyses were carried out with a TA Instrument SDT Q600 apparatus. A few milligrams of catalytic powder was put in an alumina crucible and heated under air from 25 °C to 900 °C with a temperature slope of 5 °C min⁻¹.

Transmission electron microscopy (TEM) measurements were carried out with a JEOL JEM 2010 (HR) with a resolution of 0.35 nm. The determination of the nanoparticle size distribution was performed with the ImageJ free software [17] and estimated from the measurement of 200–300 isolated nanoparticles to have acceptable statistical samples.

X-ray diffraction (XRD) patterns were recorded on a Bruker D 5005 Bragg-Brentano (θ – θ) diffractometer operated with a copper tube powered at 40 kV and 40 mA (CuK α_1 = 1.5406 Å). Measurements were performed from $2\theta = 15^\circ$ to $2\theta = 90^\circ$ in step mode, with steps of 0.06° and a fixed acquisition time of 10 s/step.

UV–visible measurements were carried out using a spectrophotometer Evolution 100 UV–visible from Thermo Electron Corp.

2.3. Electrochemical studies of the Pt/C, Ru/C and PtRu/C catalysts

Electrochemical measurements were carried out in a standard three electrode electrochemical cell at room temperature with a reversible hydrogen electrode (RHE) as the reference electrode and a glassy carbon plate as the counter electrode. The support electrolyte was a 0.5 M H₂SO₄ (Suprapur, Merck) solution in ultra pure water. Methanol electrooxidation experiments were carried out in N₂-saturated support electrolyte containing 0.1 M methanol (Absolute Puriss. ≥99.8%, Sigma–Aldrich).

The working electrode is prepared by deposition of a catalytic ink on a 0.071 cm² Glassy carbon disk according to a method

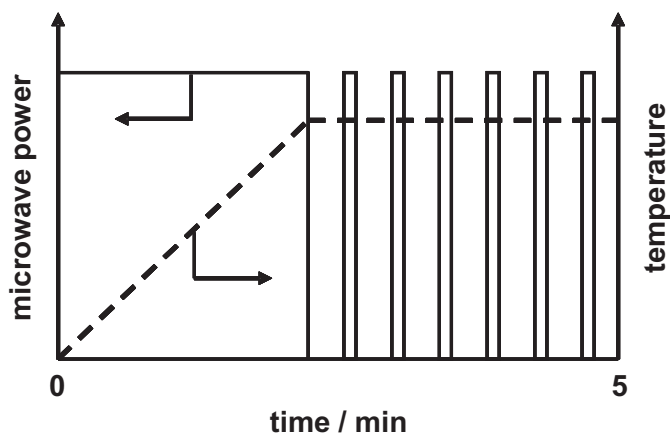


Fig. 1. Schema of the microwave sequence and of the temperature change as a function of time in course of the synthesis procedure.

proposed by Gloagen et al. [18]. Catalytic ink is composed of 5 mg of catalytic powder dissolved into 0.5 mL of ultra pure water and 0.1 mL of Nafion[®] solution (5 wt% in water and aliphatic alcohol solution from Aldrich). After 30 min homogenization in an ultrasonic bath, a volume of 3 μ L of catalytic ink is deposited from a syringe onto a fresh polished glassy carbon substrate, yielding 25 μ g of catalytic powder, i.e. 5 μ g of metal on the electrode. The solvent is then evaporated in a stream of ultra pure nitrogen at room temperature.

Cyclic voltammograms and CO stripping measurements are carried out using a Model 362 Scanning Potentiostat from Princeton Applied Research.

Infrared spectra were obtained by using the SNIFTIRS (Subtractively Normalized Interfacial Fourier Transform Infra Red Spectroscopy) method. The working electrode potential was modulated between two potential values (E_i and E_f) according to a square wave signal. The reflectivity was obtained at two electrode potentials (frequency of potential modulation: 0.025 Hz) and resulted from the co-addition of 128 interferograms 30 times at each potential. Final spectra were calculated as:

$$\frac{\Delta R}{R} = \frac{R_{E_f} - R_{E_i}}{R_{E_i}} \quad (1)$$

where E_i is the initial and E_f the final potential of the modulation and $\Delta E = E_f - E_i = 0.2$ V is kept constant. In this case, a negative peak means the production of species and a positive band indicates the consumption of species at the electrode surface.

For the in situ IR measurements, the working electrode was prepared in the same way as for cyclic voltammetry measurements.

3. Results and discussion

The synthesis of catalysts was performed under continuous microwave irradiation at a power of 1600 W until reaching the desired reaction temperature, and then microwave pulses were applied to maintain it. Fig. 1 gives a schema of the microwave sequence and of the temperature change as a function of time in course of the synthesis procedure. However, the minimal temperature at which the metal salt reduction can occur, as well as the synthesis time for the complete reduction of metal salt, is not known *a priori*. In order to determine the reduction temperature of Pt and Ru salts, UV–visible spectroscopy was used, since it has previously been shown that UV–visible spectrometry was an efficient tool to follow the Pt and PtRu colloidal formation process [19,20]. For this purpose, the spectra recorded after the heating of a H_2PtCl_6 or RuCl_3 /ethylene glycol/NaOH reaction mixture by microwave irradiation at different temperature for 5 min were compared to those recorded before microwave irradiation. It was found that the reduction of P^{4+} ions by ethylene glycol occurred as soon as 100 $^\circ\text{C}$, in agreement with previous works [14,19]. Indeed, in Fig. 2A the shape of the UV–visible spectrum before microwave irradiation is different to that recorded after microwave irradiation at 100 $^\circ\text{C}$ for 5 min over the available wavelength range. The shape of this latter spectrum, displaying strong absorption increasing gradually from ca. 700 nm towards lower wavelengths, is typical of that of a colloid [21], whereas the absorption feature at low wavelengths in the spectrum recorded before the Pt salt reduction reaction corresponds likely to the bottom of the absorption peak related to ligand-to-metal charge transfer in PtCl_6^{2-} ion (peak centred at ca. 260 nm [22]). In the case of the ruthenium salt reduction by ethylene glycol under microwave irradiation (Fig. 2B), changes in the UV–visible spectra related to the reduction of Ru^{3+} ions by ethylene glycol into Ru^0 started only to be observed at 130 $^\circ\text{C}$. In the literature, it is proposed that the formation of Ru nanoparticles

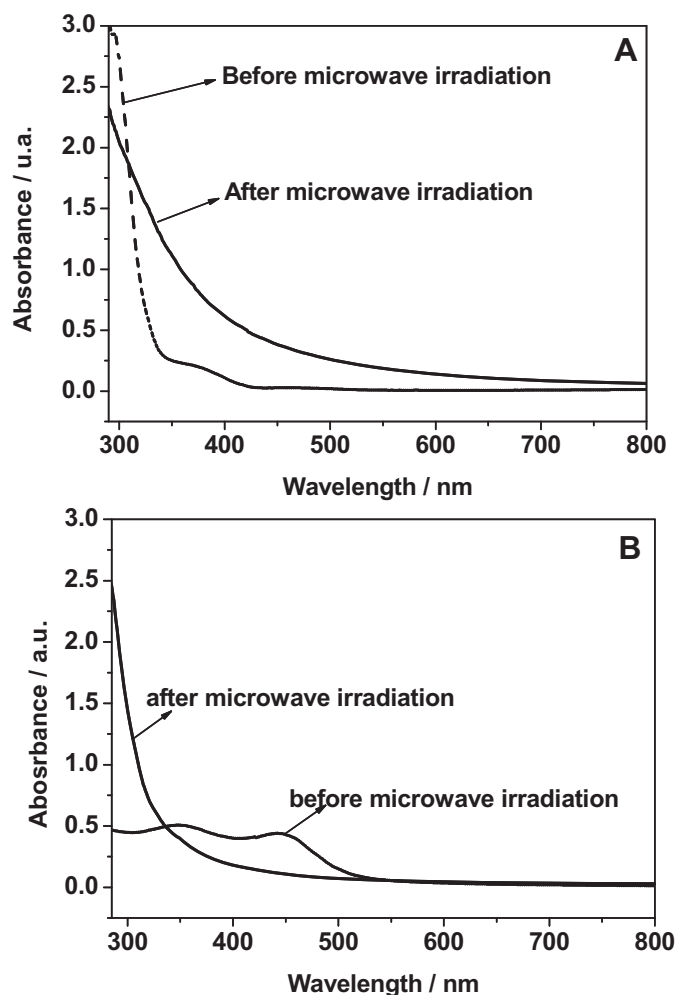


Fig. 2. UV–visible spectra recorded before and after 5 min microwave irradiation at 100 $^\circ\text{C}$ for Pt and at 130 $^\circ\text{C}$ for Ru.

gives rise to a new peak at 280 nm, which position and shape depends on duration of microwave heating [23]. The higher activation temperature needed for the reduction of Ru^{3+} ions than that for the reduction of Pt^{4+} ions can be explained by the fact that the redox potential of Ru^{3+}/Ru ($E^0 = 0.84$ V) is much lower than that of Pt^{4+}/Pt ($E^0 = 1.41$ V). However, to achieve the coreduction of platinum and ruthenium salts for synthesizing PtRu/C catalyst with a nominal Pt/Ru ratio of 1/1, it has been necessary to applied at temperature of at least 160 $^\circ\text{C}$. It appeared then that the activation energy for the formation of the bimetallic material was higher than that for the formation of the pure metal particles.

The combination of the UV–visible results with TGA measurements (Table 2) indicated that the whole metallic salts were reduced after 5 min microwave irradiation under the considered synthesis conditions. This fast reduction allows also proposing that the Pt/Ru ratio in the bimetallic catalysts is likely close to the nominal one.

Table 2

Metal loading on carbon support, particles size and Scherrer length as determined by TGA, TEM and XRD measurements, respectively.

	Metal loading (TGA)/wt.%	d (TEM)/nm	L_v (XRD)/nm
Pt/C	20	3.0 ± 0.5	3.5
Ru/C	18	(<1.5)	–
Pt ₁ Ru ₁ /C	20	2.5 ± 0.5	2.8

The synthesized carbon supported catalysts were examined by TEM. Fig. 3 shows TEM images of Pt (20 wt%)/C (A), Ru (20 wt%)/C (B) and Pt₁Ru₁ (20wt%)/C (C) samples. All samples display a homogeneous repartition of metallic particles on the carbon support. Assuming a spherical shape of the metallic clusters, the mean particle sizes could be evaluated according to the following relation:

$$\bar{d} = \frac{\sum_{i=1}^n n_i d_i}{n} \quad (2)$$

where n_i , d_i , and n are the number of particles of diameter d_i , the diameter of particles and the total number of particles, respectively. The determination of the mean catalyst particle size has been made for each catalytic powder and is given in Table 2. In the case of the pure ruthenium catalyst (Fig. 3B), the contrast of Ru on carbon is low and the particles have very small diameters, lower than 1.5 nm. The determination of the mean size was difficult to perform. Higher mean particle size was found for the pure Pt/C (ca. 3.0 nm). The Pt₁Ru₁/C sample displayed an intermediate mean particle size of ca. 2.5 nm between those of both pure metals.

XRD patterns of Pt/C, Ru/C and Pt₁Ru₁/C are represented in Fig. 4. The diffraction pattern was analysed by the method of Levenberg–Marquardt, using a Voigt fit by means of a computer refinement program (Fityk free software [24]). All diffraction patterns recorded on Pt-containing catalysts display the typical diffraction peaks of the fcc structure of platinum, whereas, the XRD pattern of the Ru displays not well defined broad peaks typical of amorphous material. The low crystallinity of the Ru/C material is convenient with the low particle size as determined by TEM. Small diffraction peaks located at ca. 35° and 55° corresponds to crystalline RuO₂ (101) and (211) orientations, respectively [25], whereas the diffraction peak at ca. 43° corresponds to metallic Ru hcp (101) orientation.

In addition to the typical diffraction peaks of the fcc structure of platinum, the XRD pattern of the Pt₁Ru₁/C catalyst also display the RuO₂ peaks at ca. 35° and ca. 55° as well as that of hcp structure of Ru at ca 43°. According to the Vegard's law for a true PtRu alloy, the value of the cell parameter should decrease when the ruthenium content increases. In other words, the diffraction peaks shift towards higher 2θ value when ruthenium is alloyed with platinum [26]. The diffraction peaks of the PtRu/C catalyst are slightly shifted towards higher 2θ values in comparison to those recorded for the Pt/C material. However, this fact can be related either to PtRu alloy formation or to size effect. But, the apparent particles sizes determined by TEM for both Pt/C and PtRu/C catalysts are very close to each other, so that size effect is probably not significant in the slight

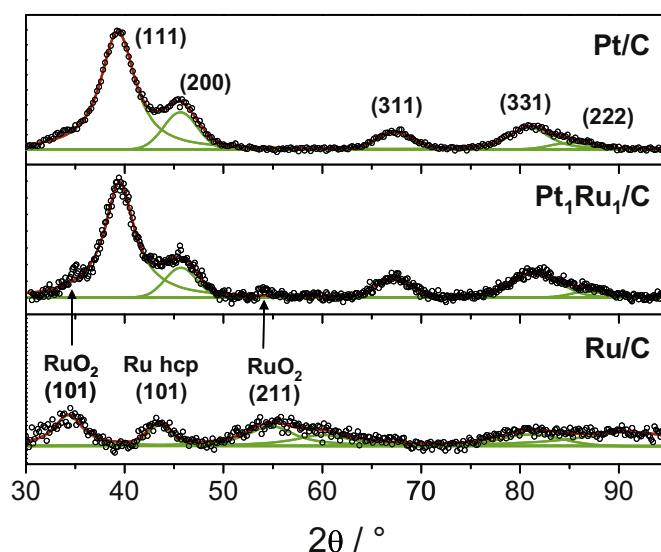


Fig. 4. XRD diffractograms in 2θ range from 30 to 90° obtained with Pt/C, Ru/C and Pt₁Ru₁/C catalysts synthesized by the polyol method activated by microwave irradiation.

diffraction peak shift. Then it was possible to determine the alloy composition by XRD [27]; the ruthenium atomic ratio was found to be ca. 21%. Therefore, it can be proposed that the structure of the Pt₁Ru₁/C catalyst consists in a mixture of fcc Pt_{0.8}Ru_{0.2} nanocrystallites, of rutile RuO₂ nanoclusters and maybe also of hcp Ru nanoclusters.

However, from the determination of the full width at half maximum (FWHM) and using the Sherrer equation [28] presented in Eq. (3), the mean size L_v for the Pt/C and PtRu/C fcc crystallites could be evaluated (Table 2).

$$L_v = \phi \frac{\lambda}{\text{FWHM} \cos \theta} \quad (3)$$

where L_v is the volume-weighted column length, ϕ is the shape factor (0.89 for spherical crystallite), λ the radiation wavelength (1.5406 Å), FWHM the full width at half maximum, and θ the angle at the maximum intensity. Crystallite sizes of 3.5 nm and 2.8 nm were determined for the Pt/C and Pt₁Ru₁/C catalysts, respectively. These values are in very good agreement with the mean particle size determined by TEM, which seems to indicate that the metallic particles are monocrystalline.

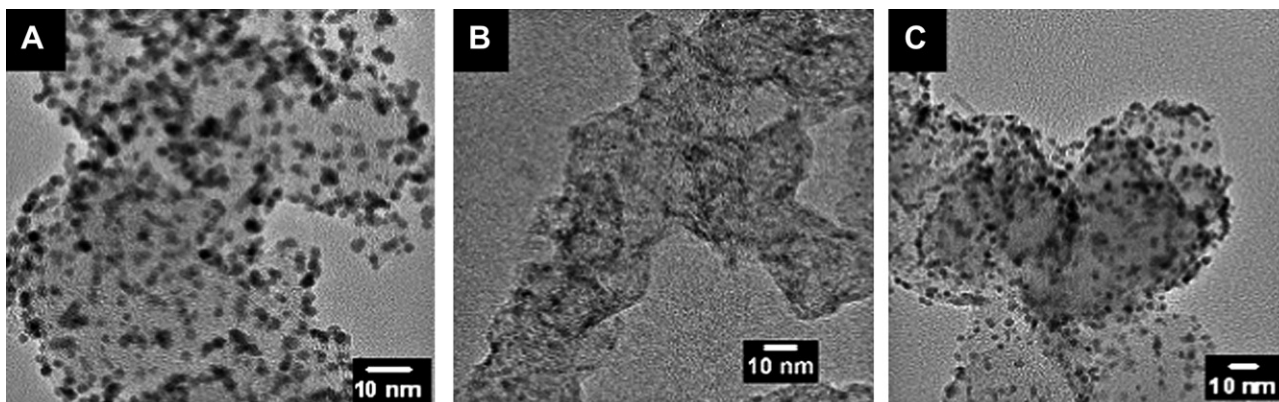


Fig. 3. TEM Photographs of (A) Pt/C, (B) Ru/C and (C) Pt₁Ru₁/C catalysts synthesized by the polyol method activated by microwave irradiation.

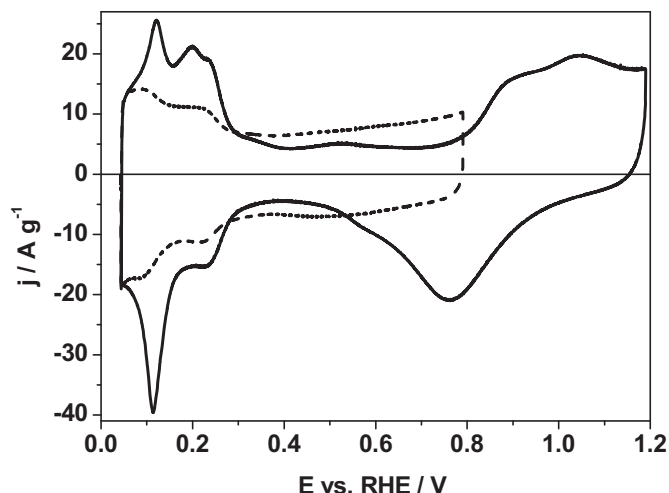


Fig. 5. Cyclic voltammograms of Pt(20 wt.%) / C (solid line) and Pt₁Ru₁(20 wt.%) / C (dashed line) synthesized by the microwave assisted polyol method, recorded at 20 mV s⁻¹, 20 °C, in a N₂-saturated 0.5 M H₂SO₄ electrolyte (*T* = 20 °C).

The active surface areas (ASA) of Pt/C and PtRu/C catalysts were determined from cyclic voltammograms (Fig. 5) by integrating the charge in the hydrogen desorption region corrected from the double layer capacity contribution [29,30], considering a charge of 210 μC per square centimetre for the desorption of a hydrogen

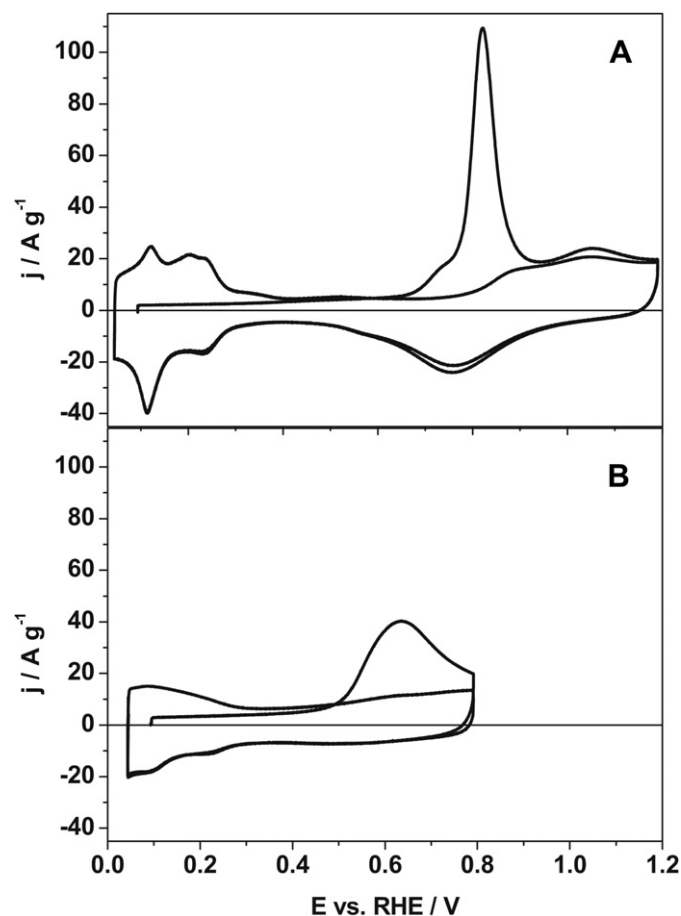


Fig. 6. CO stripping voltammograms of (A) Pt(20 wt.%) / C and (B) Pt₁Ru₁(20 wt.%) / C recorded at 20 mV s⁻¹, 20 °C, in N₂-saturated 0.5 M H₂SO₄ electrolyte.

monolayer from a smooth platinum surface [31,32]. Measurements are carried out in a N₂-saturated electrolyte at a scan rate of 20 mV s⁻¹ between 0.05 V and 1.2 V vs. RHE for Pt/C and 0.05 V and 0.8 V vs. RHE for PtRu/C. The latter upper limit potential was used in order to avoid dissolution of the ruthenium from the surface. Typical voltammogram of surface clean Pt/C and PtRu/C were recorded from which active surface areas of ca. 80 m² g⁻¹ and 30 m² g⁻¹ were found for Pt/C and PtRu/C, respectively.

CO stripping measurements were used in order to obtain information on structure, morphology and activity of nanoparticles [33–36]. For this purpose, CO surface saturation of platinum catalysts was performed at 0.1 V vs. RHE for 5 min. Before CO stripping measurements recorded by cyclic voltammetry at a potential scan rate 20 mV s⁻¹ (Fig. 6), CO was removed from the electrolyte bulk by N₂ bubbling for 15 min, under potential control at 0.1 V. For the Pt/C catalyst (Fig. 6A), the complete disappearance of the current peaks in the hydrogen desorption region (from 0.05 V to 0.4 V vs. RHE) of the first voltammetric cycle shows that the platinum surface is completely blocked by the presence of adsorbed CO. Then, the oxidation of adsorbed CO into CO₂ is responsible for the positive current peaks in the potential range from 0.65 V to 1.0 V vs. RHE. In the negative going potential scan, current peaks in the

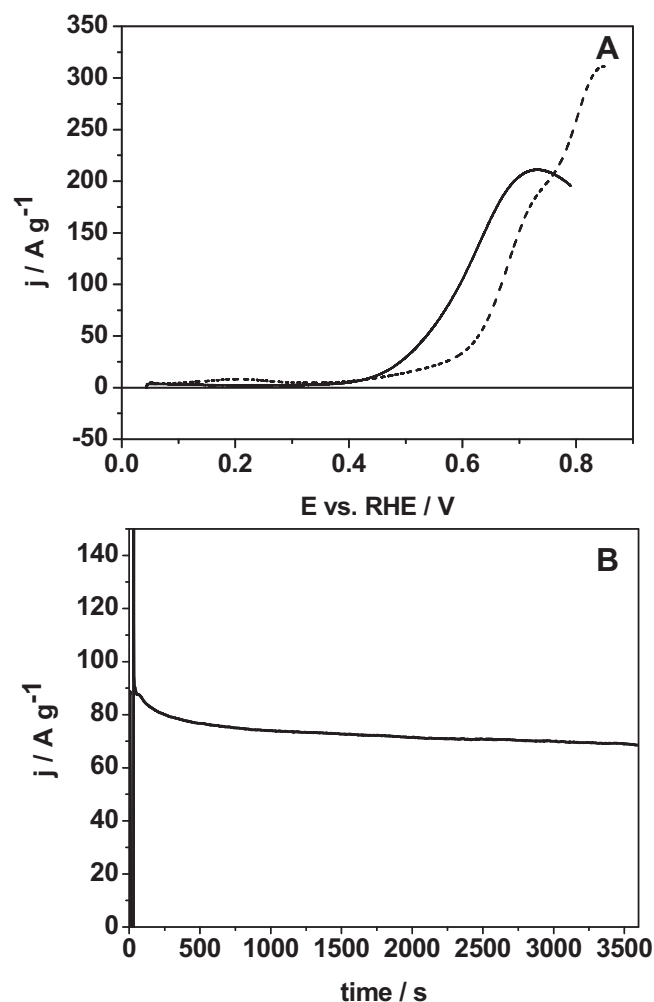


Fig. 7. (A) *j*(*E*) polarization curves recorded on Pt(20 wt.%) / C (dashed line) and on Pt₁Ru₁(20 wt.%) / C (solid line) at 5 mV s⁻¹ in N₂-saturated 0.5 M H₂SO₄ electrolyte containing 1.0 M methanol (*T* = 20 °C). (B) Chronoamperometry curve recorded on Pt₁Ru₁(20 wt.%) / C in N₂-saturated 0.5 M H₂SO₄ electrolyte containing 1.0 M methanol (*T* = 20 °C) at 0.6 V vs. RHE.

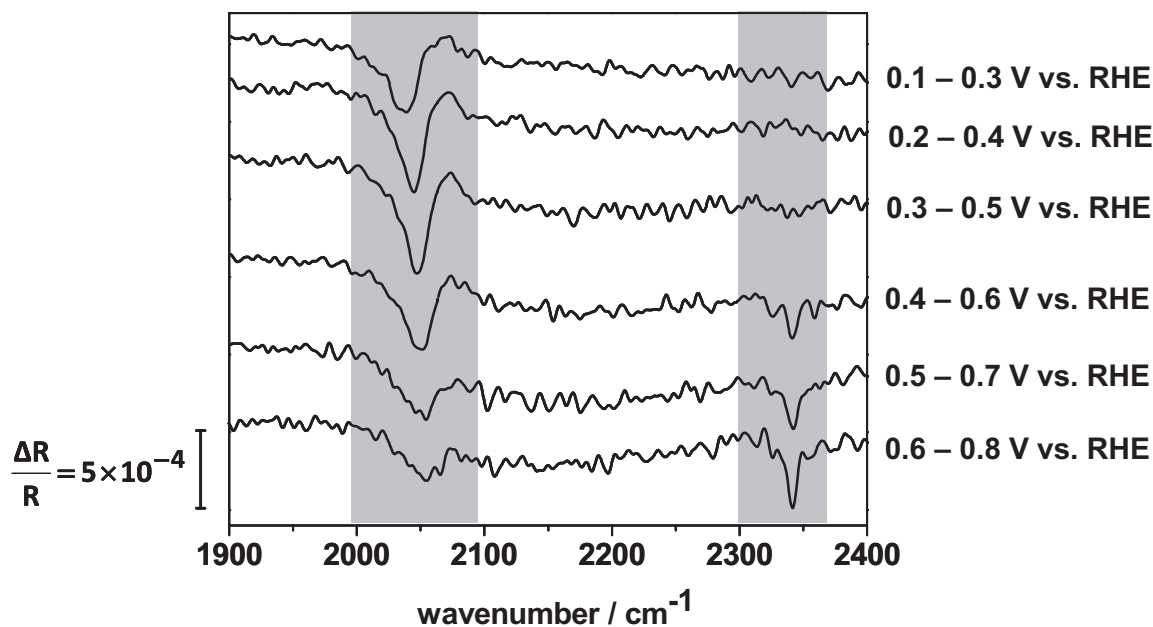


Fig. 8. SNIFTIR spectra recorded during the electrooxidation of 1.0 M methanol in 0.5 M H_2SO_4 on $\text{Pt}_1\text{Ru}_1(20 \text{ wt.}\%)/\text{C}$.

hydrogen adsorption region appeared and the second cyclic voltammogram is typical of a clean Pt/C catalyst, which indicates that adsorbed CO was totally removed from the platinum surface during the first voltammetric cycle. From the determination of the charge involved for the oxidation of the adsorbed CO, the same active surface area value as from the H_{upd} region of ca. $80 \text{ m}^2 \text{ g}^{-1}$ could be determined considering a charge of $420 \mu\text{C}$ per square centimetre for the desorption of a CO monolayer from a smooth platinum surface, which is an indication of the cleanliness of the catalyst surface. With the PtRu catalyst (Fig. 6B), the onset potential of CO_{ads} oxidation is shifted by ca. 0.2 V towards lower potentials compared with that of Pt/C catalyst, as the result of the presence of ruthenium at the material surface [37]. The active surface area calculated from the charge involved for the oxidation of the CO saturating layer is ca. $57 \text{ m}^2 \text{ g}^{-1}$. This value is almost twice higher than that calculated from the H_{upd} region. The discrepancy in the ASA values determined from H_{upd} region and from CO stripping experiment can be explained by the ability of ruthenium atoms to adsorb CO [38]. By comparing the active surface area values calculated from H_{upd} region and CO stripping measurement, and assuming that hydrogen does not adsorb on Ru sites and that CO is linearly adsorbed on both metal sites, it can be proposed that the Pt/Ru surface atomic surface composition could be close to the catalyst nominal Pt/Ru atomic ratio (1/1).

Now, let us focus on methanol oxidation at Pt/C and $\text{Pt}_1\text{Ru}_1/\text{C}$ catalysts. The polarisation curves recorded in presence of 1.0 M methanol in the support electrolyte is given in Fig. 7A. The onset potential of methanol oxidation is ca. 0.35 V vs RHE at $\text{Pt}_1\text{Ru}_1/\text{C}$, i.e. 0.2 V before that at platinum catalyst, which is agreement with result obtained with PtRu catalysts prepared by other colloidal methods [39] under the same experimental conditions. The $\text{Pt}_1\text{Ru}_1/\text{C}$ catalyst displayed higher catalytic activity towards methanol oxidation from 0.35 V vs. RHE to ca. 0.65 V vs. RHE. For higher potentials, the pure platinum supported catalyst becomes the more active one. From this potential, platinum is able to activate water and is no longer poisoned by adsorbed CO species; therefore this material becomes more active for methanol electrooxidation, than platinum–ruthenium catalyst [40]. The maximum mass current density of ca. $200 \text{ A g}_{\text{metal}}^{-1}$ at ca. 0.7 V was achieved with the $\text{Pt}_1\text{Ru}_1/\text{C}$

C catalyst. The chronoamperometry curve recorded at 0.6 V at a $\text{Pt}_1\text{Ru}_1/\text{C}$ catalyst in the presence of 1.0 M MeOH in the support electrolyte is given in Fig. 7B. Initially a current drop is observed, but it stabilizes to a constant mass current density value (ca. $70 \text{ A g}_{\text{metal}}^{-1}$) after a short time.

Both CO stripping and methanol electrooxidation experiments emphasize the well-known role of ruthenium, i.e. allowing the bifunctional mechanism at lower potential than on pure platinum [41,42]. Ruthenium brings at lower potentials than platinum the OH species necessary to complete the oxidation of adsorbed CO into CO_2 , making the bimetallic catalyst more active than Pt/C catalyst from 0.35 V to 0.7 V vs. RHE.

Fig. 8 shows SNIFTIR spectra recorded between 1900 cm^{-1} and 2400 cm^{-1} at the $\text{Pt}_1\text{Ru}_1/\text{C}$ catalytic surface with 1.0 M methanol. The absorption bands located between 2030 and 2055 cm^{-1} are assigned to linearly bonded CO (CO_{L}) [43]. No additional typical CO absorption band around 1950 cm^{-1} is visible, which could be assigned to bridge-bonded CO (CO_{B}) species [44]. The CO_{L} band appears in the first potential modulation between 0.1 and 0.3 V vs. RHE, indicating that methanol chemisorption and dehydrogenation to form adsorbed CO takes place at very low potentials on $\text{Pt}_1\text{Ru}_1/\text{C}$ catalyst. The intensity of this band first increases with the increase of potential to reach a maximum in the second and third modulations. Then, it starts to decrease from the fourth modulation, for which an absorption band located at 2345 cm^{-1} corresponding to interfacial CO_2 [43,44] starts to be observed. In addition, the CO_{L} absorption band first undergo a red shift as the average potential modulation increases, and then, from the third potential modulation, a blue shift, which are due to a combination of the Stark effect (red shift) [45] with a coverage-dependent shift of the CO infrared band (blue shift) [46].

4. Conclusion

In this contribution, we developed an industrially scalable method for the synthesis of Pt/C and PtRu/C catalysts for DMFC application. First, the method is based on a polyol route which uses inexpensive solvent (ethylene glycol), does not need the presence of surfactant and is very easy to implement. Second, instead of

using traditional thermal activation, the activation by microwave irradiation allows fast synthesis, lower energy consumption and uniform heating. The PtRu/C catalyst displayed the nominal metal loading, particle size of ca. 2.5–3.0 nm and was composed of a Pt/Ru alloy in interaction with Ru and RuO₂ clusters. Such structure gives a high activity towards CO and methanol electrooxidation to the Pt₁Ru₁/C catalyst prepared by this method. In order to improve the synthesis procedure and the catalytic performance of PtRu/C catalysts prepared by microwave assisted polyol method, the future study will focus on the effect of batch temperature and of Pt/Ru nominal composition.

Acknowledgement

This work could be realized thanks to the Sandwich PhD Fellowship Programme 2011 of the French Embassy in India.

This work was presented in 6th Asian conference on Electrochemical Power Sources held on Jan 5–8, 2012 at Chennai, Tamilnadu, India.

References

- [1] W.R. Grove, *Phil. Mag.* 21 (1842) 417.
- [2] K.H. Choi, H.S. Kim, T.H. Lee, *J. Power Sources* 75 (1998) 230.
- [3] C. Coutanceau, A. Rakotondrainibe, A. Lima, E. Garnier, S. Pronier, J.M. Léger, C. Lamy, *J. Appl. Electrochem.* 34 (2004) 61.
- [4] A. Caillard, C. Coutanceau, P. Brault, J. Mathias, J.-M. Léger, *J. Power Sources* 162 (2006) 66.
- [5] L. Dubau, C. Coutanceau, E. Garnier, J.-M. Léger, C. Lamy, *J. Appl. Electrochem.* 33 (2003) 419.
- [6] F. Vigier, C. Coutanceau, A. Perrard, E.M. Belgsir, C. Lamy, *J. Appl. Electrochem.* 34 (2004) 439.
- [7] H.S. Oh, J.G. Oh, H. Kim, *J. Power Sources* 183 (2008) 600.
- [8] J. Guo, G. Sun, S. Shiguo, Y. Shiyu, Y. Weiqian, Q. Jing, Y. Yushan, X. Qin, *J. Power Sources* 168 (2007) 299.
- [9] F. Fievet, J.P. Lagier, B. Blin, B. Beaudoin, M. Figlarz, *Solid State Ionics* 32–33 (1989) 198.
- [10] C. Bock, C. Paquet, M. Couillard, G.A. Botton, B.R. MacDougall, *J. Am. Chem. Soc.* 126 (2004) 8028.
- [11] Z. Liu, L.M. Gan, L. Hong, W. Chen, J.Y. Lee, *J. Power Sources* 139 (2005) 73.
- [12] C. Grolleau, C. Coutanceau, F. Pierre, J.M. Léger, *J. Power Sources* 195 (2010) 1569.
- [13] B.M. Babić, Lj. M. Vračar, V. Radmilović, N.V. Krstajić, *Electrochim. Acta* 51 (2006) 3820.
- [14] E. Lebègue, S. Baranton, C. Coutanceau, *J. Power Sources* 196 (2011) 920.
- [15] S.A. Galema, *Chem. Soc. Rev.* 26 (1997) 233.
- [16] M. Tsuji, M. Hashimoto, Y. Nishizawa, M. Kubokawa, T. Tsuji, *Chem. Eur. J.* 11 (2005) 440.
- [17] W.S. Rasband, Image J, U.S. National Institutes of Health, Bethesda, Maryland, USA, <http://imagej.nih.gov/ij/>, 1997–2011.
- [18] F. Gloaguen, N. Andolfatto, R. Durand, P. Ozil, *J. Appl. Electrochem.* 24 (1994) 863.
- [19] Z. Zhou, W. Zhou, S. Wang, G. Wang, L. Jiang, H. Li, G. Sun, Q. Xin, *Catal. Today* 93–95 (2004) 523.
- [20] Z. Liu, X.Y. Ling, X. Su, J.Y. Lee, *J. Phys. Chem. B* 108 (2004) 8234.
- [21] D.N. Furlong, A. Launikonis, W.H.F. Sesse, L.V. Sanders, *J. Chem. Soc., Faraday Trans. 1* 80 (1984) 571.
- [22] T. Teranishi, M. Hosoe, T. Tanaka, M. Miyake, *J. Phys. Chem. B* 103 (1999) 3818.
- [23] R. Harpeness, Z. Peng, X. Liu, G. V-Pol, Y. Koltypin, A. Gedanken, *J. Colloid. Interf. Sci.* 287 (2005) 678.
- [24] M. Wojdyr, *J. Appl. Cryst.* 43 (2010) 1126.
- [25] A. Devadas, S. Baranton, T.W. Napporn, C. Coutanceau, *J. Power Sources* 196 (2011) 4044.
- [26] P. Vogel, H. Britz Bönemann, J. Rothe, J. Hormes, *J. Phys. Chem. B* 101 (1997) 11029.
- [27] C.A. Angelucci, M. D'Villa Silva, F.C. Nart, *Electrochim. Acta* 52 (2007) 7293.
- [28] P. Scherrer, *Nachr. Ges. Wiss. Göttingen, Math.-Phys. Klasse* 26 (1918) 98.
- [29] C. Coutanceau, M.J. Croissant, T. Napporn, C. Lamy, *Electrochim. Acta* 46 (2000) 579.
- [30] C. Grolleau, C. Coutanceau, F. Pierre, J.M. Léger, *Electrochim. Acta* 53 (2008) 7157.
- [31] V.S. Bakotzky, Y.B. Vassilyev, *Electrochim. Acta* 12 (1967) 1323.
- [32] N.M. Markovic, B.N. Grgur, P.N. Ross, *J. Phys. Chem. B* 101 (1997) 5405.
- [33] F. Maillard, S. Schreier, M. Hanzlik, E.R. Savinova, S. Weinkauff, U. Stimming, *Phys. Chem. Chem. Phys.* 7 (2005) 385.
- [34] M. Arenz, K.J.J. Mayrhofer, V. Stamenkovic, B.B. Blizanac, T. Tomoyuki, P.N. Ross, N.M. Markovic, *J. Am. Chem. Soc.* 127 (2005) 6819.
- [35] A. Cuesta, A. Couto, A. Rincón, M. Pérez, A. López Cudero, C. Gutiérrez, *J. Electroanal. Chem.* 586 (2006) 184.
- [36] A. López Cudero, J. Solla Gullón, E. Herrero, A. Aldaz, J.M. Feliu, *J. Electroanal. Chem.* 644 (2010) 117.
- [37] M. Watanabe, S. Motoo, *J. Electroanal. Chem.* 60 (1975) 275.
- [38] L. Dubau, F. Hahn, C. Coutanceau, J.M. Léger, C. Lamy, *J. Electroanal. Chem.* 554–555 (2003) 407.
- [39] C. Coutanceau, S. Brimaud, L. Dubau, C. Lamy, J.-M. Léger, S. Rousseau, F. Vigier, *Electrochim. Acta* 53 (2008) 6865.
- [40] H.A. Gasteiger, N. Markovic, P.N. Ross, E.J. Cairns, *J. Electrochem. Soc.* 141 (1994) 1795.
- [41] M. Watanabe, S. Motoo, *J. Electroanal. Chem.* 75 (1960) 267.
- [42] M. Watanabe, S. Motoo, *J. Electroanal. Chem.* 75 (1960) 275.
- [43] K. Kunimatsu, *J. Electroanal. Chem.* 140 (1982) 205.
- [44] B. Beden, F. Hahn, S. Juanito, C. Lamy, J.-M. Léger, *J. Electroanal. Chem.* 225 (1987) 215.
- [45] B. Beden, C. Lamy, A. Bewick, K. Kunimatsu, *J. Electroanal. Chem.* 121 (1981) 343.
- [46] C. Rice, Y.Y. Tong, E. Oldfield, A. Wieckowski, F. Hahn, F. Gloaguen, J.-M. Léger, C. Lamy, *J. Phys. Chem. B* 104 (2000) 5803.